THE JOURNAL OF BIOLOGICAL CHEMISTRY VOL. 285, NO. 34, pp. 26641–26651, August 20, 2010

c-Src-mediated Phosphorylation of Thyroid Hormone Receptor-interacting Protein 6 (TRIP6) Promotes Osteoclast Sealing Zone Formation[S]

Received for publication, March 4, 2010, and in revised form, May 17, 2010 Published, JBC Papers in Press, June 14, 2010, DOI 10.1074/jbc.M110.119909

Brooke K. McMichael, Stephanie M. Meyer, and Beth S. Lee[1]

From the Department of Physiology and Cell Biology, The Ohio State University College of Medicine, Columbus, Ohio 43210

Osteoclasts resorb bone through the formation of a unique attachment structure called the sealing zone. In this study, a role for thyroid hormone receptor-interacting protein 6 (TRIP6) in sealing zone formation and osteoclast activity was examined. TRIP6 was shown to reside in the sealing zone through its association with tropomyosin 4, an actin-binding protein that regulates sealing dimensions and bone resorptive capacity. Suppression of TRIP6 in mature osteoclasts by RNA interference altered sealing zone dimensions and inhibited bone resorption, whereas overexpression of TRIP6 increased the sealing zone perimeter and enhanced bone resorption. Treatment of osteoclasts with lysophosphatidic acid (LPA), which phosphorylates TRIP6 at tyrosine 55 through a c-Src-dependent mechanism, caused increased association of TRIP6 with the sealing zone, as did overexpression of a TRIP6 cDNA bearing a phosphomimetic mutation at tyrosine 55. Further, LPA treatment caused increases in osteoclast fusion, sealing zone perimeter, and bone resorptive capacity. In contrast, overexpression of TRIP6 containing a nonphosphorylatable amino acid residue at position 55 severely diminished sealing zone formation and bone resorption and suppressed the effects of LPA on the cytoskeleton. LPA effects were mediated through its receptor isoform LPA(2), as indicated by treatments with receptor-specific agonists and antagonists. Thus, these studies suggest that TRIP6 is a critical downstream regulator of c-Src signaling and that its phosphorylation is permissive for its presence in the sealing zone where it plays a positive role in osteoclast bone resorptive capacity.

Discovered in 1996 through a screen of proteins that interact with thyroid hormone receptors in a ligand-specific manner (1), thyroid hormone receptor-interacting protein 6 (TRIP6)[2] belongs to the zyxin focal adhesion/nuclear shuttling family that also includes the lipoma preferred partner, Ajuba, and LIMD1 (2, 3). Similar to other proteins in this family, TRIP6 contains three C-terminal LIM domains, a proline-rich N terminus of unknown function, a nuclear export signal, but no known nuclear import signal (4). LIM domains are double zinc finger domains of ~50–60 amino acids that function in protein-protein interaction and have been found to be involved in regulating transcription and cytoskeletal organization (2, 3). Most LIM family proteins do not have enzymatic domains and function mainly as adaptor proteins.

In the cell types studied to date, TRIP6 has been detected primarily at focal adhesion plaques with lower abundance in nuclei. Mutation of the nuclear export signal causes accumulation of TRIP6 in nuclei (4), as does synthesis of a naturally occurring form of TRIP6 that lacks this N-terminal sequence (5). Early studies indicated that along with a nuclear export sequence, TRIP6 contains multiple transactivation domains yet does not have the ability to bind DNA directly (4). TRIP6 was found to be a co-regulator of the v-Rel transcription factor (6), as well as of transcription factors AP-1 and NF-κB (5). More recently, TRIP6 has been shown to modulate focal adhesions by forming complexes with $p130^{Cas}$, paxillin, FAK, and c-Src, among others (7). The adaptor abilities/multifunctional binding of TRIP6 can be partially attributed to its three C-terminal LIM domains.

Osteoclasts, giant multinucleated cells of monocyte origin, are terminally differentiated cells responsible for regulating bone density by degrading, or resorbing, bone. Osteoclastogenesis is induced by osteoblastic expression of receptor activator for nuclear factor κB ligand (RANKL), which recruits and binds monocytic precursors, thus stimulating osteoclast formation (8). Once differentiated, osteoclasts tightly attach to bone and resorb the organic matrix and hydroxyapatite mineral beneath the cell through secretion of hydrochloric acid and proteases, particularly cathepsin K (9).

Osteoclast attachment to bone occurs through a unique structure called the sealing zone. The sealing zone is composed in part of tightly packed actin filaments that form a ring at the ventral side of a polarized cell. Integrins associated with the sealing zone facilitate tight attachment to bone to create an acidic, protease-rich microenvironment at the bone surface that promotes its resorption. The osteoclast sealing zone therefore is essential to osteoclast function. When cultured on non-bone substrates, mature osteoclasts form peripheral belts of podosomes, foot-like adhesion structures that contains a short F-actin core that undergoes rapid turnover (10, 11). Podosomes and sealing zones are distinct but structurally related adhesion structures that contain a multitude of actin regulatory proteins and signaling molecules, including the nonreceptor tyrosine kinase c-Src (11). c-Src is ubiquitously expressed in mammalian tissues, but its importance to osteoclast function was under-

[S] The on-line version of this article (available at http://www.jbc.org) contains supplemental Figs. S1–S5.

[1] To whom correspondence should be addressed: Dept. of Physiology and Cell Biology, 304 Hamilton Hall, 1645 Neil Ave., Columbus, OH 43210. Fax: 614-292-4888; E-mail: lee.2076@osu.edu.

[2] The abbreviations used are: TRIP, thyroid hormone receptor-interacting protein; LPA, lysophosphatidic acid; RANKL, receptor activator for nuclear factor κB ligand; Tm, tropomyosin; GST, glutathione *S*-transferase; siRNA, small interfering RNA; RT, reverse transcription.

scored by generation of a knock-out mouse whose major phenotype was osteopetrosis caused by formation of nonfunctioning osteoclasts (12). Although multinucleated osteoclasts were generated in the absence of c-Src, these cells lacked the ability to form sealing zones and resorb bone (12–14). Of relevance to this study, c-Src has been shown to phosphorylate tyrosine 55 of TRIP6 in NIH 3T3 cells when stimulated with lysophosphatidic acid (15).

Naturally occurring soluble lysophosphatidic acid (LPA) functions in a variety of biological processes including proliferation, migration, muscle contraction, tumor cell invasion, inhibition of differentiation, and cell survival (reviewed in Ref. 16). LPA functions through cell surface signaling in a G protein-dependent manner. LPA has been shown to be involved in short term responses (*e.g.* changes in motility and cell shape) and long term responses (activation of gene transcription). LPA exerts its effects through at least five known receptors that show extensive overlap in their association with G proteins (reviewed in Ref. 17). The LPA(1) and LPA(2) receptors both couple to $G_{\alpha 12/13}$, $G_{\alpha q/11}$, and $G_{\alpha i/o}$. LPA(3) can couple with only the latter two of these G proteins, whereas LPA(5) couples only with $G_{\alpha 12/13}$, and $G_{\alpha q/11}$. LPA(4) is unique in coupling to $G_{\alpha s}$ in addition to $G_{\alpha 12/13}$, $G_{\alpha q/11}$, and $G_{\alpha i/o}$. TRIP6 previously was shown to bind LPA(2), facilitating its c-Src-mediated phosphorylation (7, 15). Current research in skeletal biology has shown that LPA affects all bone cell types. LPA was shown to be a chemotactic agent for osteoblast MC3T3-E1 cells while stimulating dendrite outgrowth of MLO-Y4 osteocytes (18, 19). In chondrocytes, LPA decreases apoptosis and promotes chondrocyte differentiation and survival (20). Recent studies have suggested that LPA stimulates osteoclasts indirectly through changes in local interleukin levels (21, 22); however, even more recent findings noted that LPA is capable of directly promoting osteoclast differentiation (23).

Previously, we showed that osteoclasts express multiple isoforms of tropomyosins, actin-binding proteins that stabilize F-actin, and found that tropomyosin 4 (Tm-4) specifically regulates both sealing zone and podosome height (24, 25). In this study, we determined that TRIP6 is associated in complexes with Tm-4. Utilizing small interfering RNA knockdowns and overexpression of TRIP6 combined with immunocytochemistry and resorption assays, we found that c-Src regulates osteoclast adhesion and resorption in part through tyrosine phosphorylation of TRIP6.

EXPERIMENTAL PROCEDURES

Reagents and Cell Culture—Mouse polyclonal antibodies against Tm-4 and TRIP6 were purchased from Abnova. Rabbit polyclonal antibodies against Tm-4 and TRIP6 were purchased from Chemicon International and Bethyl Laboratories, respectively. Mouse monoclonal antibodies were used for detection of FLAG (F-1804, Sigma), β-actin (Abcam), and phosphotyrosine residues (PY69; BD Transduction Laboratories). The mouse IgG clone MOPC-21 was obtained from Sigma. Lysophosphatidic acid was purchased from Cayman Chemical Company and used at 2 μM. Murine osteoclasts were generated either from RAW264.7 macrophages (American Type Culture Collection) or murine bone marrow cells. Osteoclast differentiation was induced by culturing precursor cells in the presence of recombinant GST-RANKL as previously described (26). RAW264.7 macrophages were plated at a density of 20,000 cells/cm^2 and cultured in Dulbecco's modified Eagle's medium with 10% fetal bovine serum and 50 ng/ml recombinant GST-RANKL. The medium was replaced on day 3 of culture and every second day thereafter for up to 6 total days of culture. For mouse bone marrow-derived osteoclasts, marrow cells were collected and incubated overnight in α-minimum essential medium with 10% fetal bovine serum plus 20 ng/ml macrophage colony-stimulating factor. The next day, nonadherent cells were collected and incubated for an additional 5–6 days in the presence of 10 ng/ml macrophage colony-stimulating factor and 50 ng/ml GST-RANKL, replacing the medium every second day for up to 6 total days of culture. Osteoclasts were identified as the cells expressing tartrate-resistant acid phosphatase and containing at least three nuclei. Further, osteoclasts were considered to have reached maturity when they were capable of forming peripheral belts of podosomes when cultured on glass, as previously defined (27).

Western Analysis and Immunoprecipitation—Western analysis was performed as previously described (28). Immunoprecipitation of ^{35}S-labeled or unlabeled protein also was performed as previously described (28, 29). Some precipitates were incubated in actin-depolymerizing G buffer (20 mM Tris-HCl, pH 7.4, 0.5 mM ATP, 0.5 mM $CaCl_2$, 0.2 mM dithiothreitol) overnight prior to running in SDS-PAGE.

Immunocytochemistry and Microscopy—Osteoclasts were prepared for immunocytochemistry by differentiating precursor RAW264.7 or marrow cells on either glass coverslips or thinly sliced ivory. Following differentiation, the cells were fixed, permeabilized, and allowed to bind antibodies as previously described (28). Primary antibodies were added in a standard polyethylene glycol blocking buffer and were detected using Alexa-labeled secondary antibodies (Invitrogen). F-actin was labeled using Alexa-conjugated phalloidin (Invitrogen). The cells were visualized using a Zeiss 510 META laser scanning confocal microscope (Campus Microscopy and Imaging Facility, The Ohio State University). Sealing zone dimensions were determined by generating Z-stack images of randomly selected cells and measuring these structures at their thickest points, as previously described (25).

RNA Interference-mediated Knockdown of TRIP6—siRNAs were designed and synthesized by Ambion (Austin, TX). siRNAs 69658, 294418, and 294419 were successfully used to demonstrate RNA and protein knockdown and are referred to in this study as siRNAs 3, 5, and 6, respectively. siRNA5 was used for all siRNA experiments, and siRNA6 was used in many experiments to confirm results. For all experiments, a nontargeting double-stranded RNA from Ambion was used as a negative control, although siRNAs homologous to siRNA5 and siRNA6 but containing point mutations also were used for confirmation. siRNA transfections were previously described (30). On day 5 of osteoclast differentiation, 75 nM of siRNA or an equal concentration of a control siRNA was transfected via Lipofectamine 2000 (Invitrogen). Bone marrow-derived osteoclasts were electroporated in siPORT buffer (Ambion) at 250 V/50 microfarads with the siRNA solution or an equal concen-

tration of a control siRNA. For immunocytochemical analysis, the cells were replated on ivory slices or glass coverslips immediately following the transfection. For RNA analysis, total cellular RNA was harvested 1–3 days after the transfection with RNA-Bee (Tel-test, Inc). For protein analysis, whole cell lysates were harvested 1–4 days post-transfection with M-PER (Pierce). Optimal knockdown was achieved 2 days post-transfection.

To determine TRIP6 mRNA expression levels by RT-PCR, primers were created that corresponded to murine sequences. The sense primer was of the sequence 5′-GATGCTGAGATAGATTCGCTCACC-3′, whereas the antisense primer was of the sequence 5′-TGCAGGGATATGTACTCCAGAAGG-3′. For an internal standard, a cDNA was created that corresponded to the expected PCR product using the primers above but contained an internal deletion of 29%, a T7 promoter element, and a tail of 15 adenosines, as previously described (25, 31). This product was transcribed *in vitro* using the MAXIscript system (Ambion), and 200 femtograms of the resulting RNA (the internal standard) was added to 1 μg of osteoclast total cellular RNA prior to reverse transcription and PCR. These reactions were performed using the Superscript first strand synthesis system from Invitrogen. The resulting RT-PCR products were run in a 2% gel and stained with ethidium bromide to visualize the relative intensities of the bands, which were measured using Quantity One software (Bio-Rad).

Bone Resorption Assays—Five days after initial RANKL stimulation, osteoclasts were transfected and immediately plated on BD BioCoat Osteologic discs (BD Biosciences) or thinly cut ivory slices as a bone substrate. Control and siRNA-treated cells were kept on the discs/bone for 3 days. The cells were removed by the addition of bleach for 5 min and several washes with water or by scraping. Bone was stained 5 min with acid hematoxylin and mounted on glass slides, and resorption was assayed by confocal microscopy. BD discs were assayed by photographing under low magnification and quantifying resorbed areas with SigmaScan Pro 5.0 software (SPSS Science). Equal numbers of images were compared among test groups. In general, marrow-derived osteoclasts were assayed on bone slices, whereas RAW264.7-derived osteoclasts were assayed on Osteologic discs. Although RAW264.7 osteoclasts are capable of resorbing bone, the pits generated do not possess clear-cut margins, making quantification of their size difficult.

Overexpression of TRIP6—A TRIP6 cDNA containing 14 bp of the 5′-untranslated region, the entire coding region, and 64 bp of the 3′-untranslated region was isolated by RT-PCR and cloned into the eukaryotic expression vector pEF6/V5-His (Invitrogen). This construct was stably transfected into RAW264.7 macrophages using Lipofectamine and Plus reagents (Invitrogen); the empty pEF6/V5-His vector was stably transfected into cells as a control. The cells were maintained in 3 μg/ml blasticidin for selection. TRIP6 mutants were created using the QuikChange XL system to create single or double point mutations at TRIP6 tyrosine 55 (Stratagene). A FLAG epitope was added to verify expression of mutants. Mutants with and without the FLAG tag were either stably overexpressed by Lipofectamine or transiently overexpressed by electroporation at 250 V/150 microfarads.

Measurements—Sealing zone measurements were made using SigmaScan Pro 5.0 software (SPSS Science) and Zeiss 510 META microscope software. 10 × 10-μm pictures were analyzed for podosome numbers. Pairwise comparison of samples was performed using two-tailed Student's t tests. Statistical comparison was deemed significant at $p < 0.05$.

RESULTS

Tropomyosin 4 Binds TRIP6—Tropomyosins are a class of helical proteins that bind actin filaments and regulate the accessibility of other proteins to the filaments. We have identified numerous tropomyosin isoforms in osteoclasts (24). One of these, Tm-4, is enriched in the actin core of podosomes and sealing zones, where it regulates the shape of these structures and affects osteoclast motility and bone resorptive capacity (25). To identify Tm-4 binding partners other than F-actin, osteoclasts were metabolically labeled, and Tm-4-containing complexes were immunoprecipitated. The *left lane* of Fig. 1*A* demonstrates several proteins precipitated in these complexes, including Tm-4 itself, β-actin, and a protein of ~50 kDa that we putatively identified as TRIP6 through published studies demonstrating Tm-4/TRIP6 interactions (32). When immunoprecipitated complexes were treated in G buffer to depolymerize microfilaments prior to SDS-PAGE analysis, the β-actin band disappeared, and only the Tm-4 and 50-kDa bands remained (Fig. 1*A*, *right lane*). These results suggest that Tm-4 directly binds the putative TRIP6 protein, as previously indicated by yeast two-hybrid analysis (32). To confirm the association of Tm-4 and TRIP6, immunoprecipitations with antibodies against Tm-4, TRIP6, or an irrelevant antibody control (MOPC) were subsequently analyzed by Western for their proposed binding partners. Fig. 1*B* confirms that TRIP6 interacts with a complex of Tm-4 and β-actin.

To determine the distribution of TRIP6 in osteoclasts, wild-type mouse bone marrow-derived or RAW264.7-derived osteoclasts were differentiated on glass or bone, immunocytochemically labeled for TRIP6 along with F-actin, and viewed under confocal microscopy. In contrast to other cell types studied to date in which TRIP6 has a strong cytoplasmic presence (4, 7, 32, 33), osteoclast TRIP6 is primarily nuclear/perinuclear but also has a minor presence in adhesion structures. Fig. 1*C* illustrates this in marrow-derived and RAW264.7-derived osteoclasts cultured on glass. In these cells, peripheral actin and nuclei were clearly labeled by anti-TRIP6 antibody. A similar distribution of TRIP6 was seen in cells on bone that generate actin-rich sealing zones. The *top row* of Fig. 1*D* shows an osteoclast with strong nuclear/perinuclear staining and a faint localization to the sealing zone. The confocal images in the *bottom row* of Fig. 1*D* are focused particularly in the sealing zone of a separate cell to determine where, within this structure, TRIP6 resides. Confocal z-sectioning shows that TRIP6 resides within the central core of the sealing zone (as indicated by the *yellow regions* in the Z-stack). This overlaps the location of Tm-4, which is distributed throughout the interior half of the this adhesion structure (25). Thus, the distributions of these proteins intersect in the sealing zone but are not identical. TRIP6 distribution also was examined in macrophages. Similar to our findings in osteoclasts, TRIP6 in macrophages also was demonstrated to be

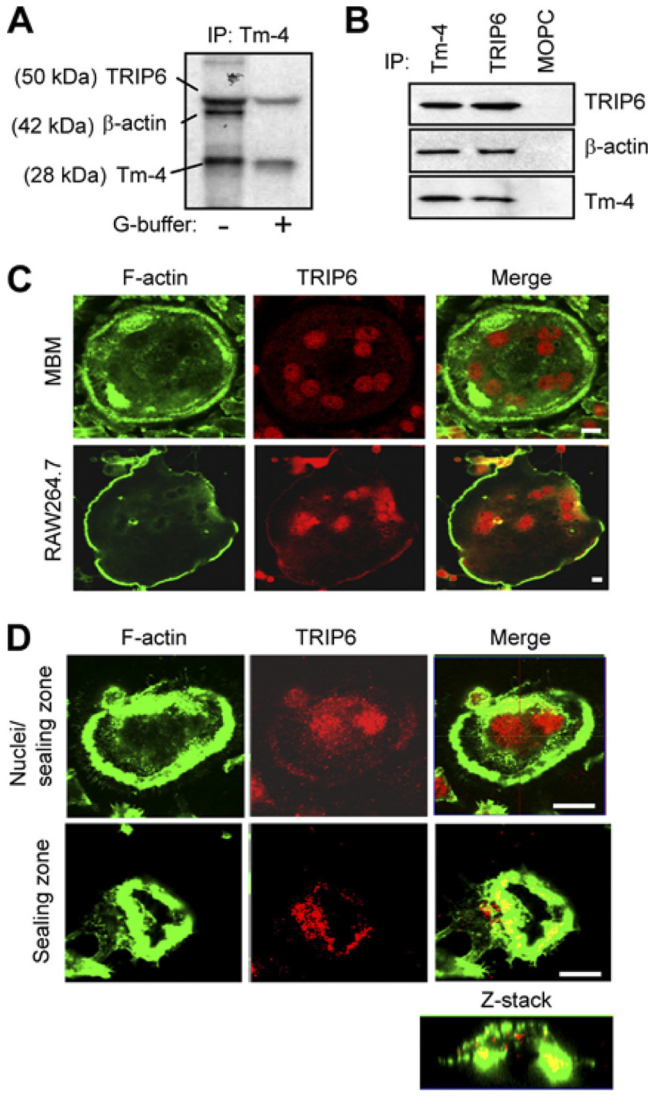

FIGURE 1. **Tropomyosin-4 binding partner TRIP6 has a nuclear and cytoplasmic distribution in osteoclasts.** *A*, immunoprecipitation (*IP*) of Tm-4 from ^{35}S-radiolabeled osteoclasts was performed under standard conditions and in the presence of G buffer to disrupt filamentous actin. *B*, immunoprecipitation from unlabeled osteoclasts followed by Western analysis was performed to confirm Tm-4/TRIP6 interactions. *C*, RAW264.7- and mouse bone marrow (*MBM*)-derived osteoclasts were plated on glass and examined by confocal microscopy for the localization of TRIP6 (*red*) and F-actin (*green*). *D*, osteoclasts were examined on bone for the localization of TRIP6 (*red*) along with F-actin (*green*). *Scale bars*, 10 μm.

primarily nuclear/perinuclear (supplemental Fig. S1). TRIP6 localization in osteoclasts suggests the potential for both nuclear and cytoskeletal functions. This study focuses only on its role in the cytoskeleton because TRIP6 previously has been shown to associate with multiple actin regulating proteins known to be essential for attachment to substrate, motility, and resistance to apoptosis.

TRIP6 Suppression Alters Sealing Zone Dimensions and Decreases Resorptive Capacity—To determine roles for TRIP6 in the osteoclast cytoskeleton, siRNAs were generated to knock down TRIP6 mRNA and protein expression. Fig. 2*A* illustrates that three siRNAs (si3, si5, and si6) were capable of suppressing TRIP6 expression in mouse bone marrow-derived osteoclasts. The *top panel* shows a competitive RT-PCR where the *upper band* represents TRIP6 mRNA, whereas the *lower band* represents an internal standard. Transfection of a nontargeting control oligonucleotide (C0) maintained normal levels of TRIP6 mRNA, whereas transfection of the specific mRNAs (si3, si5, and si6) caused its loss. Accordingly, siRNA treatment of osteoclasts caused a loss of TRIP6 protein (Fig. 2*A*, *middle panel*), whereas β-actin levels stayed constant (Fig. 2*A*, *bottom panel*). Fig. 2*B* demonstrates that siRNAs si5 and si6 also knocked down TRIP6 expression in RAW264.7-derived osteoclasts. This figure further shows that two mutated versions of si5 and si6 (C5 and C6) did not affect TRIP6 expression. Multiple such experiments indicated that TRIP6 mRNA and protein routinely could be decreased by 60–70% during siRNA treatment in both osteoclast cell models. Fig. 2*C* shows that knockdown of TRIP6 expression can be detected immunocytochemically in both marrow-derived macrophages and osteoclasts and that its loss occurs equivalently from cytoskeletal and nuclear/perinuclear compartments.

To determine how suppression of TRIP6 affects cytoskeletal organization in osteoclasts, mature osteoclasts were treated with either control oligonucleotides or TRIP6 siRNAs and examined on bone. Labeling of cells with fluorescent phalloidin to demarcate the sealing zones revealed that TRIP6 suppression resulted in increased sealing zone width and loss of sealing zone height (viewed by confocal z-sectioning). These results are illustrated graphically in Fig. 3*A*. The perimeters of these actin rings were unchanged (data not shown). Because knockdown of TRIP6 has been associated with changes in activity of Rho family GTPases (33, 34) and RhoA plays a critical role in osteoclast sealing zone formation (35, 36), we tested whether knockdown of TRIP6 in osteoclasts resulted in altered RhoA activity. Fig. 3*B* demonstrates that siRNA-mediated knockdown resulted in a ~3.5-fold increase in active RhoA. Further, TRIP6 knockdown was accompanied by changes in resorptive capacity. Bone resorption was measured by two methods. First, cells were cultured on ivory, and the resulting resorption pit depth, area, and length were measured by confocal microscopy. Fig. 3 (*C* and *D*) shows that resorptive pits generated by siRNA-treated osteoclasts on ivory were shallower and covered less surface area than pits generated by control-treated cells. However, pits made by TRIP6-suppressed cells were more linear and covered greater length. In a second method, the cells were cultured on discs thinly layered with apatite (BD Biosciences), which also promote sealing zone formation and resorption (37). Although pit depth cannot be measured using these discs because of the thinness of the apatite layer, the average area per resorbed clearing and the number of clearings can be assessed. Fig. 3*E* shows by this assay that TRIP6 siRNA-treated cells also generated clearings/pits with areas ~50% less than controls, whereas the number of clearings/pits increased. These results confirm that TRIP6 plays a role in the resorptive capacity of osteoclasts. We also examined how TRIP6 suppression affected podosome belts of mature osteoclasts cultured on glass. Although the adhesion structures (podosome rings/belts) made by osteoclasts on glass or plastic are not identical to sealing zones on bone, they share many structural and functional similarities (11). Although suppression of TRIP6 caused an increase in sealing zone widths in cells on ivory (Fig. 3*A*), suppression of TRIP6

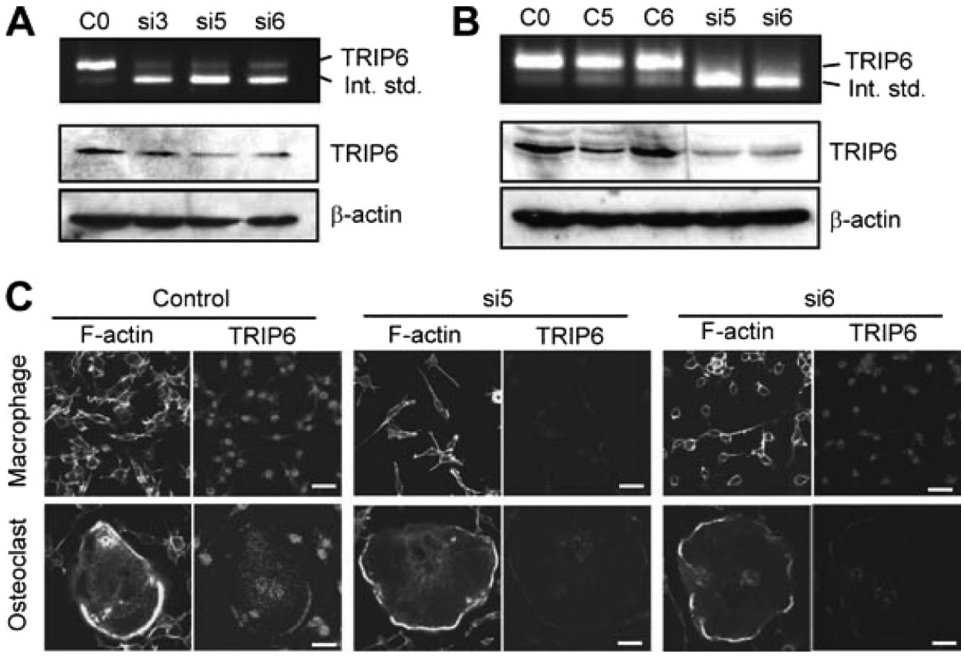

FIGURE 2. **RNA interference-mediated knockdown of TRIP6.** *A*, *top panel*, competitive RT-PCR demonstrates knockdown of TRIP6 in marrow-derived osteoclasts by any of three specific siRNAs (si3, si5, and si6) but not by a nontargeting control oligonucleotide (C0). *Middle panel*, loss of corresponding TRIP6 protein levels is demonstrated. *Bottom panel*, β-actin levels are shown as a loading control. *B*, similar experiments were performed to show knockdown in RAW264.7 osteoclasts, except that two additional controls (C5 and C6) were included to show specificity of the si5 and si6 siRNAs. *C*, siRNA-mediated knockdown of TRIP6 is demonstrated in mouse bone marrow macrophages and osteoclasts by immunolabeling and confocal microscopy. TRIP6 levels decrease throughout the cell. *Scale bars*, 10 μm.

caused an increase in the number of podosomes, resulting in widened podosome belts. These data are presented in supplemental Fig. S2.

TRIP6 Overexpression Alters Sealing Zone Formation and Increases Resorptive Capacity—As a complement to the previous studies in which TRIP6 levels were suppressed in osteoclasts, we generated stably transfected RAW264.7 cell lines that overexpress TRIP6. Fig. 4*A* shows a Western blot of four clonal lines that overexpress TRIP6 and one control line transfected with empty vector. A 2–4-fold increase in TRIP6 protein was achieved (Fig. 4*A*). Overexpression of TRIP6 also was evident by immunocytochemistry (Fig. 4*A*, *lower panels*) and did not prevent these macrophage lines from differentiating into osteoclasts in the presence of RANKL. In differentiated osteoclasts, TRIP6 was located in a normal distribution between the cytoskeletal adhesion structures and a nuclear/perinuclear location. To determine how TRIP6 overexpression affected sealing zones, these cells were cultured on bone and labeled with fluorescent phalloidin. Fig. 4*B* illustrates that sealing zones of TRIP6-overexpressing cells were altered in dimension. Satisfyingly, whereas TRIP6-suppressed cells produced sealing zones of greater width than controls, TRIP6-overexpressing cells produced sealing zones of lesser width. However, height was not altered, but sealing zone perimeter was increased. Finally, TRIP6-overexpressing cells were assayed for resorptive capacity. Resorption assays were carried out only on apatite discs because we have determined that RAW264.7-derived osteoclasts on ivory form pits with indistinct margins, making quantification difficult.[3] As shown in Fig. 4*C*, TRIP6-overexpressing cells produced larger resorbed areas than control cells. This result is in contrast to TRIP6-suppressed cells, which produced smaller resorbed areas. However, like TRIP6-suppressed cells, the overexpressers also showed a greater number of clearings. We also examined podosome belts of osteoclasts cultured on glass. Perhaps not unexpectedly, TRIP6-overexpressing cells generated belts containing fewer podosomes than controls, in contrast to the siRNA-treated cells, which generated more podosomes (supplemental Fig. S3).

LPA Stimulates Association of TRIP6 with the Cytoskeleton and Enhances Cell Fusion and Resorptive Capacity—Previous studies by Lai *et al.* (15) demonstrated that LPA induces c-Src-mediated phosphorylation of TRIP6 at tyrosine 55 in fibroblasts. Because c-Src plays an essential role in arrangements of the osteoclast cytoskeleton and sealing zone formation (13), we examined the effects of LPA on osteoclast activity. LPA was added overnight to fully differentiated osteoclasts, and cells were prepared for immunocytochemistry to reveal F-actin and TRIP6 distribution. As demonstrated in Fig. 5*A* (*left panels*), LPA-treated cells generated sealing zones that showed a more intense labeling for TRIP6 than vehicle-treated controls. In addition, TRIP6 co-precipitated with the sealing zone protein Tm-4 to a greater extent in LPA-treated cells than in control cells (Fig. 5*A*, *right panel*). Treatment of cells with the c-Src inhibitor PP2 in addition to LPA inhibited this increased association. These results demonstrate that a c-Src-mediated event is responsible for the increased cytoskeletal association of TRIP6 produced by from LPA stimulation. To confirm that LPA stimulates c-Src-mediated phosphorylation of TRIP6 in osteoclasts, the cells were treated with LPA or vehicle for 15 min, and TRIP6 was immunoprecipitated and probed with a phosphotyrosine-specific antibody. As shown in Fig. 5*B*, LPA treatment did not cause an increase in total TRIP6 levels but did cause an increase in TRIP6 tyrosine phosphorylation. These results are consistent with those in other cell models in which LPA stimulated Tyr-55 phosphorylation of TRIP6, resulting in increased association with the cytoskeleton (15).

To further explore the effects of LPA on osteoclast morphology and function, mature osteoclasts were treated with LPA overnight, fixed, and treated with fluorescent phalloidin to

[3] B. K. McMichael, unpublished data.

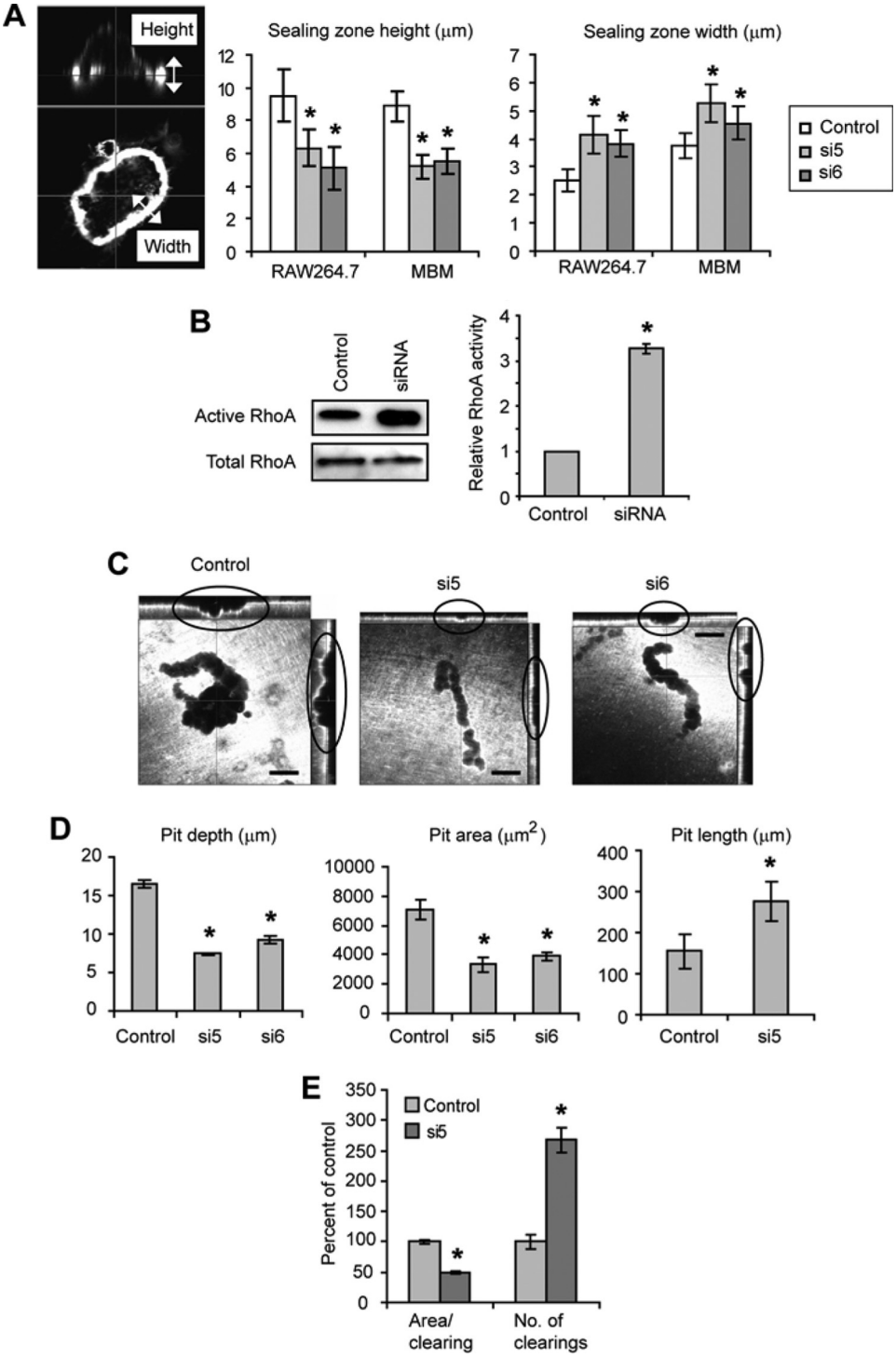

FIGURE 3. **Decreased TRIP6 levels alter sealing zone dimensions and resorption.** *A*, osteoclast sealing zones were labeled with fluorescent phalloidin, and sealing zone heights and widths were measured, as indicated in the microscopic image. Graphical data are expressed as the means ± S.D. Four independent experiments were performed in which at least 12 sealing zones were measured for each sample. The *asterisks* indicate statistically significant differences from controls. For all of the measurements, $p < 0.004$. *B*, multiple Western blots to test RhoA activation, such as those on the *left*, were quantified to produce the graphical data on the *right* ($n = 3$; $p < 1 \times 10^{-5}$). *C*, marrow-derived osteoclasts were cultured on ivory, and resorption pits were visualized using acid hematoxylin staining coupled with confocal z-sectioning. *Scale bars*, 40 μm. *D*, pits generated from marrow-derived osteoclasts on ivory were quantified from three independent experiments in which at least 12 pits were assessed per sample. For all measurements, $p < 0.004$. *E*, siRNA-treated osteoclasts on apatite discs showed similar resorptive activity to osteoclasts on ivory by generating smaller but more clearings. For comparisons of control to siRNA-treated cells, six independent experiments were performed in which at least 10 clearings were measured per sample ($p < 0.01$).

demarcate adhesion structures. Fig. 5*C* (*left panel*) shows a low magnification view of such cells cultured on bone. As is evident, LPA-treated cells demonstrated sealing zones with a greater perimeter than controls. This finding was quantified for both RAW264.7- and marrow-derived osteoclasts in the *middle panel* of Fig. 5*C*. We have previously demonstrated that the average sealing zone perimeter increases with the average number of osteoclast nuclei (28). To determine whether LPA increased fusion of osteoclasts, resulting in cells with larger sealing zones, the average nuclear number was determined in LPA-treated and control cells. As shown in the *right panel* of Fig. 5*C*, LPA significantly increased the average nuclear number and, thus, cell fusion. Further, overnight LPA treatment also caused an increase in the area of resorption pits/clearings produced by these osteoclasts, as demonstrated by cells cultured on bone (Fig. 5*D*) or apatite discs (Fig. 5*E*). The results in this figure demonstrate that LPA produces profound effects on osteoclast cytoskeletal morphology and function, including inducing phosphorylation of TRIP6.

Loss of TRIP6 Phosphorylation Abolishes Sealing Zone Formation and Resorption—Because treatment of osteoclasts with LPA promoted a change in the distribution of TRIP6, we examined whether this change was attributable to c-Src-mediated phosphorylation at tyrosine 55. Plasmids expressing C-terminal FLAG-tagged versions of wild-type TRIP6, a tyrosine 55 to phenylalanine mutant (Y55F), or a tyrosine 55 to aspartic acid mutant (Y55D) were transiently transfected into mature osteoclasts, and their phenotypes were observed on bone. Transient transfections resulted in 2–4-fold changes in total TRIP6 expression (supplemental Fig. S4). Fig. 6*A* demonstrates that wild-type TRIP6-FLAG was distributed between the sealing zone and nuclei, consistent with endogenous TRIP6 distribution. In contrast, cells expressing the Y55F-FLAG mutant (which

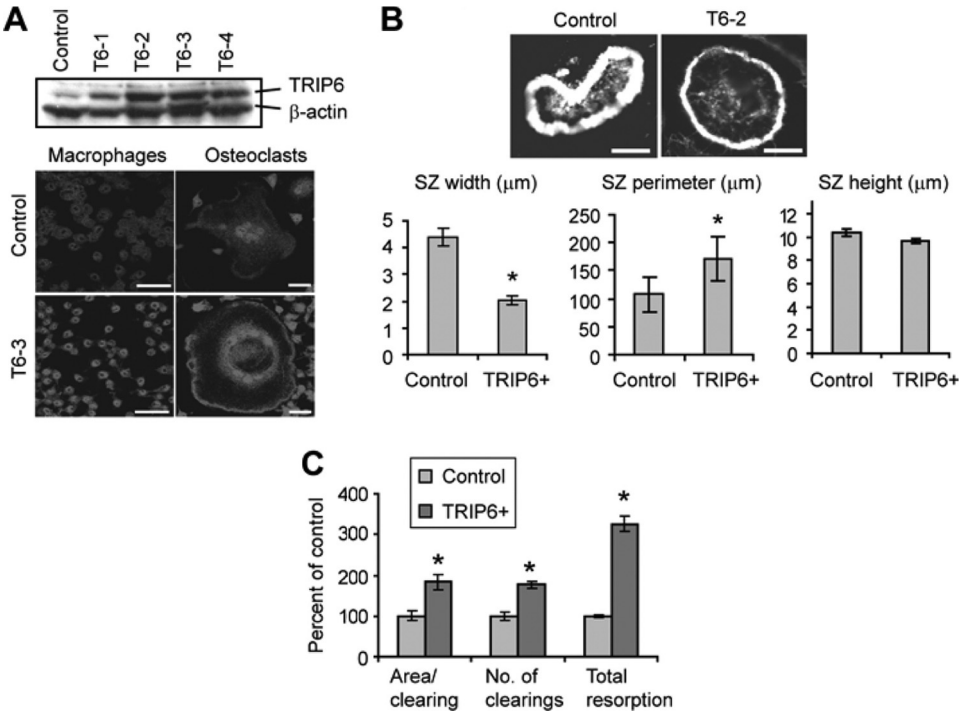

FIGURE 4. **Overexpression of TRIP6 decreases sealing zone width and increases resorption.** *A*, *top panel*, Western analysis demonstrates the overexpression of TRIP6 in four stably transfected RAW264.7 clones (*T6-1* to *T6-4*) relative to a clone transfected with empty vector. The Western also shows β-actin bands as loading controls. Clones T6-2 and T6-3 were used for all experiments. *Bottom panel*, immunolabeling and confocal microscopy of cells on glass illustrate that the overexpressing clones present a normal distribution of TRIP6 (in adhesion structures and nuclear/perinuclear). *Scale bars*, 10 μm. *B*, *top panel*, TRIP6-overexpressing osteoclasts cultured on bone show distinctive thinning of sealing zone width. *Bottom panel*, quantification of several measurements demonstrates decreased sealing zone width and increased perimeter but no change in height. The graphical data are expressed as the means ± S.D. from six independent experiments in which at least 12 sealing zones were measured per sample. The *asterisks* indicate statistical significance ($p < 0.003$). *Scale bars*, 10 μm. *C*, control and TRIP6-overexpessing cells were assayed for resorptive capacity on apatite discs. TRIP6-overexpressing clones demonstrated increases in clearing size, clearing number, and overall resorption. Three independent experiments were performed in which at least 60 clearings were measured. For all measurements, $p < 0.002$.

cannot be phosphorylated) made very poor sealing zones, and the exogenous TRIP6 was most heavily distributed in nuclei. Finally, the cells expressing the phosphomimetic Y55D-FLAG mutant made typical sealing zones, and the exogenous TRIP6 mutant was distributed evenly throughout the sealing zone and cytoplasm with little concentration in nuclei. The presence of TRIP6 in the cytoplasm may be attributable to saturation of the exogenous protein in the sealing zone. Nonetheless, these results, along with the data in Fig. 5, suggest that TRIP6 phosphorylation at tyrosine 55 is required for its presence in the sealing zone, and a lack of phosphorylatable TRIP6 negatively affects the ability of the cell to form a sealing zone. Similar results were obtained in stably transfected osteoclasts; cells overexpressing wild-type TRIP6 were capable of forming sealing zones, whereas the Y55F mutants generated these structures poorly and had altered morphology (supplemental Fig. S5).

To determine how phosphorylation at tyrosine 55 affects bone resorption, the cells transiently expressing wild-type TRIP6-FLAG or the Y55F-FLAG and Y55D-FLAG mutants were cultured on apatite discs. Fig. 6*B* illustrates that relative to TRIP6-FLAG-expressing cells, osteoclasts expressing the mutant forms produced similar numbers of resorbed areas, but the Y55F-FLAG mutants produced clearings of less area, whereas the Y55D-FLAG mutants produced larger clearings. These results are consistent with phosphorylatable TRIP6 playing a positive role in sealing zone formation and resorptive capacity. To further demonstrate that TRIP6 phosphorylation plays a critical role in LPA-stimulated effects on the cytoskeleton, LPA or vehicle was added to cells transiently expressing Y55F-FLAG or Y55D-FLAG TRIP6 cDNAs or empty vector as a control. As expected, LPA caused an increase in the sealing zone perimeter in wild-type osteoclasts, whereas cells expressing the Y55D-FLAG cDNA produced large sealing zones in either the absence or the presence of LPA (Fig. 6*C*). This finding suggests that the effects of LPA on sealing zone size may be mediated primarily through TRIP6 phosphorylation. In contrast, Y55F-FLAG-transfected cells produced small, poorly delineated sealing zones in the absence of LPA. A small increase in sealing zone size was stimulated by LPA, most likely on the endogenous wild-type TRIP6 present in these cells. However, in the general absence of TRIP6 phosphorylation, LPA could not exert its normal effects on sealing zone formation. Together, these data suggest TRIP6 as the primary mediator of LPA-induced sealing zone rearrangements.

LPA Stimulates TRIP6-mediated Cytoskeletal Changes through the LPA(2) Receptor—Finally, we wished to identify the LPA receptor(s) involved in producing these cytoskeletal changes. TRIP6 had previously been shown to bind the C-terminal tail of receptor LPA(2), but not LPA(1) or LPA(3), in HEK 293T cells (7). Further, this interaction was shown to be required for LPA-mediated anti-apoptotic signaling in the same cell line (38). To determine which receptor might play a role in osteoclast cytoskeletal arrangements, we employed commercially available antagonists and agonists of LPA receptor isoforms. As previously demonstrated in Fig. 5, treatment of mature osteoclasts with LPA overnight caused increases in osteoclast fusion and sealing zone size. Fig. 7*A* shows that cells treated with LPA in the presence of LPA1/LPA3 antagonist Ki16425 are also increased in osteoclast fusion and sealing zone size, similar to cells treated with LPA only. This result suggests that the LPA effects demonstrated in this study are not due to the action of either of these receptors. Although an LPA(2) receptor-specific antagonist does not exist, an agonist, FAP12, is available. Fig. 7*B* illustrates that treatment of mature osteoclasts with LPA or FAP12 produces similar effects on cell fusion and sealing zone perimeter, indicating the role of LPA(2) in these changes. Finally, to confirm that the effects of LPA on cell fusion are c-Src-dependent, LPA was added to osteoclasts in the presence or the absence of the c-Src

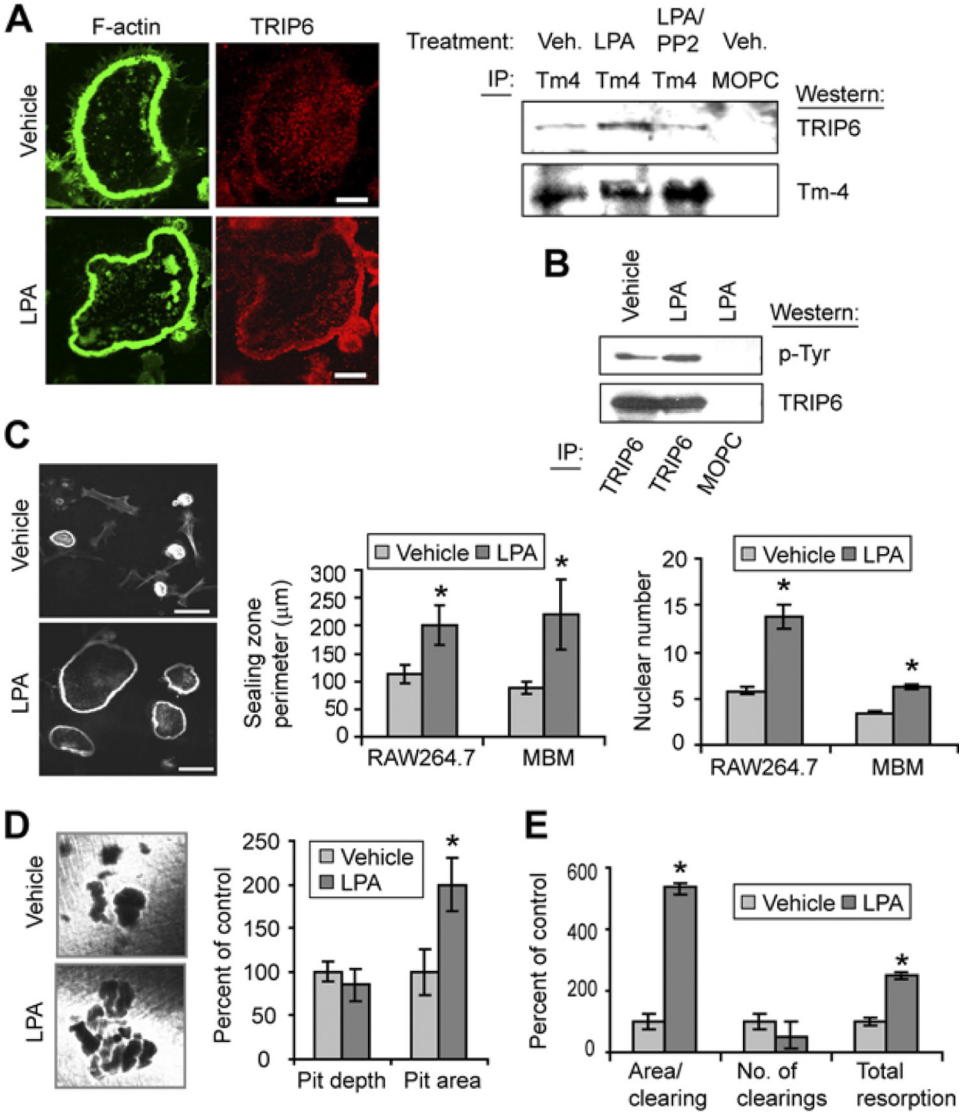

FIGURE 5. **LPA induces increased osteoclast size and activity along with phosphorylation of TRIP6 and alterations in its distribution.** *A*, *left panel*, labeling of TRIP6 (*red*) and F-actin (*green*) in cells on bone demonstrates that LPA treatment caused TRIP6 to concentrate into the sealing zone. *Scale bars*, 10 μm. *Right panel*, Tm-4 was immunoprecipitated (*IP*) from cells treated with vehicle (*Veh.*), LPA, or LPA + c-Src inhibitor PP2. Antibody MOPC was used as a negative control for Tm-4 binding. The resulting complexes were separated by SDS-PAGE and immunoblotted with antibodies to TRIP6 or Tm-4. *B*, LPA treatment of osteoclasts for 15 min caused an increase in the phosphorylation of TRIP6. Immunoprecipitation was performed using an anti-TRIP6 antibody or MOPC, and the resulting precipitates were Western blotted for either TRIP6 or phosphotyrosine residues. *C*, *left panel*, labeling of F-actin in osteoclasts on bone demonstrates the effects of LPA on sealing zone and cell size. *Scale bars*, 100 μm. *Right panel*, quantification of sealing zone perimeter and cell fusion (nuclear number) demonstrates that LPA increases these properties in both RAW264.7- and marrow-derived osteoclasts. The data are expressed as the means ± S.D. from three to six separate experiments in which at least 24 cells were assessed. For all measurements, $p < 2 \times 10^{-4}$. *D*, LPA treatment of marrow-derived osteoclasts on bone increases resorption pit area ($p < 2 \times 10^{-4}$) but not depth ($p = 0.07$). Three independent experiments were performed in which at least 10 pits were measured. *E*, similarly, LPA treatment of RAW264.7-derived osteoclasts on apatite discs caused increases in the area of clearing. Three independent experiments were performed in which at least 75 clearings were measured ($p < 2 \times 10^{-5}$).

inhibitor PP2. As demonstrated in Fig. 7*C*, PP2 completely abolished the LPA-stimulated effects on cell fusion. The results demonstrate that LPA(2) is the primary receptor involved in the stimulation of osteoclast cytoskeletal rearrangements and that its effects work through a c-Src-dependent mechanism.

DISCUSSION

We previously identified tropomyosin 4 as a mediator of osteoclast sealing zone generation and resorptive capacity (25). Although our data indicate that tropomyosin 4 directly associates with few proteins, TRIP6, one of its few binding partners, has been shown so far to bind over 50 different proteins (39). These binding partners include transcription factors and cytoskeletal elements, placing TRIP6 in a class of proteins that can regulate both cell adhesion and gene expression. Our findings that TRIP6 plays an important role in osteoclast adhesion are in keeping with studies in other cell types such as HeLa, where TRIP6 was found to be essential for stress fibers and mature focal adhesions (33). Although osteoclasts generate alternate and unique actin-based structures, it is clear that TRIP6 similarly promotes cytoskeletal arrangements that favor cell activation.

Experiments in which TRIP6 was either knocked down or overexpressed suggest that this multifunctional protein generally produces a positive effect on the ability of osteoclasts to degrade bone. That is, knockdown of TRIP6 diminished the size of resorptive pits, whereas overexpression of TRIP6 increased them. However, because TRIP6 has both nuclear and cytoskeletal distributions in osteoclasts, global manipulations of TRIP6 levels do not distinguish between potential transcriptional and cytoskeletal roles for the protein. Indeed, our preliminary data suggest that nuclear TRIP6 may dampen osteoclast formation and survival (not shown). In contrast, LPA treatment of osteoclasts caused increased TRIP6 levels only in the cytoskeletal compartment, allowing better interpretation of the role of TRIP6 in the osteoclast cytoskeleton. LPA-mediated increases of TRIP6 in adhesion structures promoted larger sealing zones and greater resorptive activity. Although LPA produces numerous effects on cellular activities, we were able to isolate its effects on TRIP6 by overexpression of cDNAs mutated in the tyrosine residue phosphorylated through the action of LPA. These results confirmed the critical role that TRIP6 plays in sealing zone formation and resorptive capacity. Further, LPA treatment caused increases in fusion of osteoclast precursors, as indicated by greater average nuclear numbers/cell. This could be

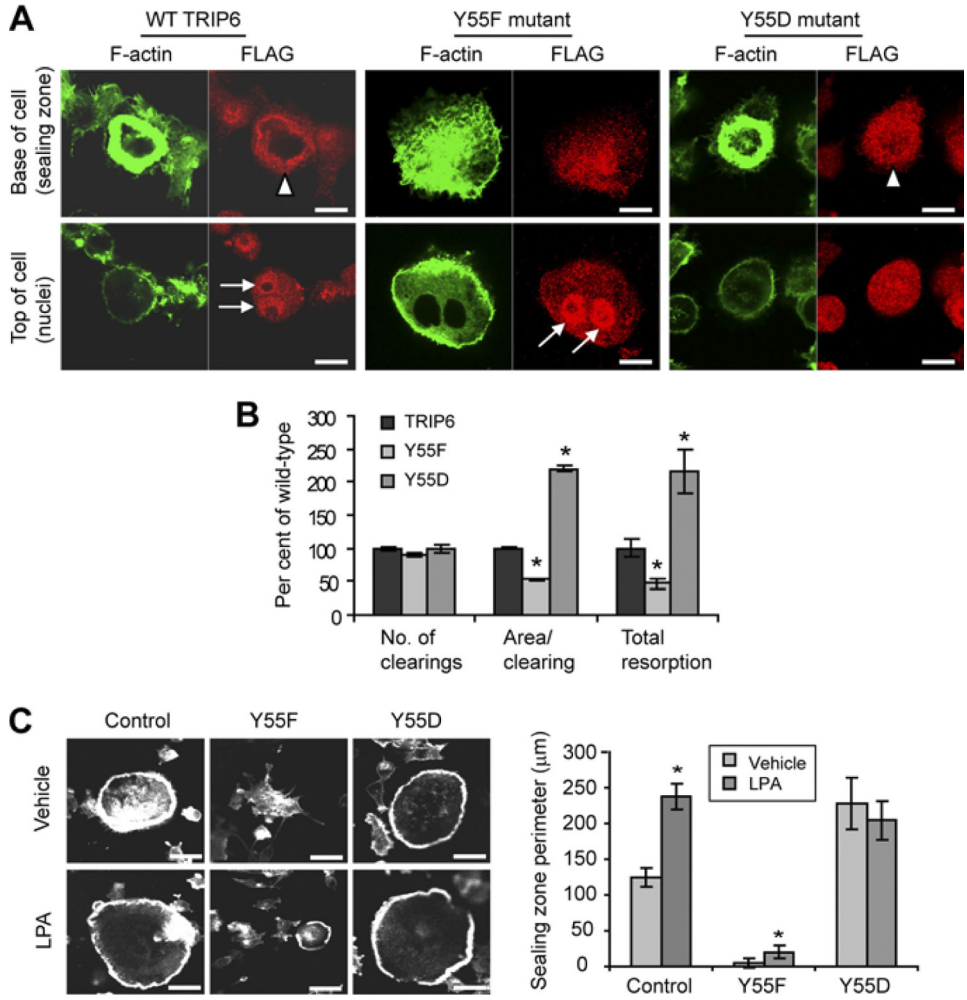

FIGURE 6. **Phosphorylation of TRIP6 at tyrosine 55 is required for sealing zone formation and resorptive capacity.** *A*, TRIP6 (*red*) and F-actin (*green*) z-sections on bone demonstrate that impaired TRIP6 phosphorylation (Y55F mutant) causes the loss of sealing zones, whereas overexpression of a Y55D (phosphomimetic) mutant still results in sealing zone formation. The nuclei are indicated by *arrows*, whereas sealing zones are indicated by *arrowheads*. *Scale bar*, 10 μm. *B*, transient overexpression of TRIP6 mutant Y55F leads to a decrease in the size of the clearings on apatite discs, whereas phosphomimetic Y55D increases the size of the clearings. Quantification is expressed as the mean ± S.D. from three independent experiments in which at least 60 clearings were measured. The *asterisks* indicate differences from wild type ($p < 3 \times 10^{-4}$). *C*, Y55F, and Y55D cDNAs were transiently overexpressed, and the resulting cells on ivory were treated with LPA for 24 h. The cells were fixed and stained with fluorescent phalloidin. As shown by photos (*left panels*) and graphically (*right panels*), LPA treatment could only very poorly compensate for the loss of sealing zones in Y55F mutants, whereas LPA caused no change in the already increased numbers of sealing zones in cells overexpressing the phosphomimetic Y55D. For photomicrographs, the *scale bars* indicate 50 μm. The *asterisks* indicate statistical differences between vehicle- and LPA-treated cells. Five independent experiments were performed in which at least 18 sealing zones were measured per sample. For control cells, $p < 3 \times 10^{-4}$; for Y55F, $p < 0.05$; for Y55D, $p = 0.40$.

a result of LPA causing cytoskeletal rearrangements that favor fusion, because we recently showed that alterations in expression of one cytoskeletal protein, myosin IIA, promote osteoclast multinucleation (28). Alternately, formation of larger osteoclasts may result from anti-apoptotic effects mediated through the receptor LPA(2), as shown in murine fibroblasts (38). Our preliminary data indicate a strong anti-apoptotic effect of LPA on osteoclasts, and studies are ongoing to define the mechanisms by which LPA generates its effects on osteoclastogenesis and function.

A major effect of cellular exposure to LPA is activation of the nonreceptor tyrosine kinase c-Src. In 1991, a knock-out mouse model for c-Src demonstrated this kinase to be essential to osteoclast function. Indeed, osteopetrosis resulting from osteoclast inactivation was found to be the unique phenotype of these mice (12). Although osteoclasts were generated by these animals, a loss of c-Src led to an absence of sealing zones and resorptive capacity (13, 14). In this study, we have identified TRIP6 as a major downstream mediator of c-Src activity that promotes sealing zone formation. Our data show that phosphorylation of Tyr-55 by c-Src promotes TRIP6 association with cytoskeletal structures and is necessary for sealing zone formation, because osteoclasts overexpressing a nonphosphorylatable TRIP6 are nearly incapable of generating these sealing zones, even when stimulated with LPA. The responses of TRIP6 to c-Src activation are reminiscent of those for one of its binding partners, the adaptor protein p130^{Cas} (32). Like TRIP6, the phosphorylation of p130^{Cas} and its association with the osteoclast cytoskeleton are c-Src-dependent (40). Studies of p130^{Cas}-null osteoclasts have been hindered because of the embryonic lethality of a global p130^{Cas} knock-out (41). However, c-Src-transformed embryonic fibroblasts, which form podosomes, have been obtained from these animals. Although p130^{Cas} did not appear to be necessary for podosome formation, its re-expression in the p130^{Cas}-deficient fibroblasts caused a dramatic induction of podosome rings and belts in these cells, structures with similarity to the sealing zone of osteoclasts. These results suggest that a complex of c-Src-phosphorylated TRIP6 and p130^{Cas} is likely to play a key role in osteoclast sealing zone formation.

In summary, our studies have identified one role of TRIP6 in osteoclasts and, in doing so, have revealed a mechanism by which LPA can directly promote osteoclast activity. These results are in contrast to published studies in which LPA was suggested to activate osteoclasts in bone through indirect means, by altering local interleukin levels (21, 22). Because these studies showed LPA to aid in the progression of osteolytic bone metastases, understanding its direct effects on osteoclasts activity may provide targets for therapy. In addition, these studies have revealed TRIP6 as a downstream

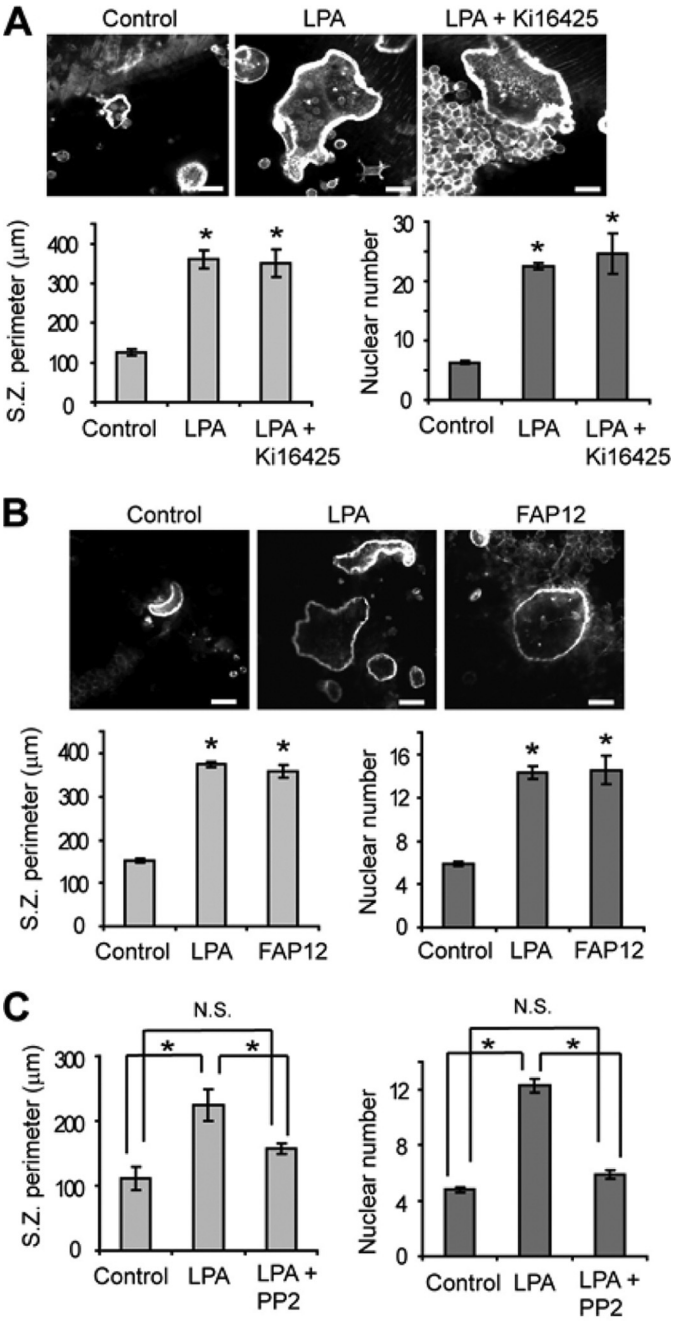

FIGURE 7. **Cytoskeletal effects of LPA are mediated through the LPA(2) receptor.** *A*, Ki16425, an antagonist of LPA receptors LPA(1) and LPA(3), does not inhibit the effects of LPA on sealing zone perimeter and osteoclast fusion. The cells in the *top panels* are labeled with fluorescent phalloidin to visualize peripheral podosome belts. *Scale bars*, 50 μm. Four independent experiments, assessing at least 12 cells/sample, are quantified and graphed in the *lower panels*. The *asterisks* indicate statistically significant differences from controls ($p < 0.01$). *B*, LPA-stimulated effects on osteoclast sealing zone perimeter and fusion are mediated through the LPA(2) receptor, because treatment with LPA(2) agonist FAP12 stimulates fusion to the same extent as LPA. In the *top panel*, the cells were labeled with fluorescent phalloidin. *Scale bars*, 50 μm. The *bottom panels* show graphical representation of four independent experiments in which at least 12 cells were assessed per sample. The *asterisks* indicate statistically significant difference from controls ($p < 1 \times 10^{-6}$). *C*, changes in the LPA-mediated sealing zone perimeter and cell fusion are c-Src-dependent, because treatment with LPA in the presence of c-Src inhibitor PP2 inhibits fusion. Three independent experiments were performed in which at least 12 cells were assessed per sample. The *asterisks* indicate $p < 0.005$. *N.S.*, not significant.

mediator of c-Src signaling in osteoclasts, which promotes numerous cytoskeletal rearrangements and resistance to apoptosis.

Acknowledgment—We thank the Campus Microscopy and Imaging Facility at the Ohio State University for continued technical advice and support.

REFERENCES

1. Lee, J. W., Choi, H. S., Gyuris, J., Brent, R., and Moore, D. D. (1995) *Mol. Endocrinol.* **9,** 243–254
2. Wang, Y., and Gilmore, T. D. (2003) *Biochim. Biophys. Acta* **1593,** 115–120
3. Zheng, Q., and Zhao, Y. (2007) *Biol. Cell* **99,** 489–502
4. Wang, Y., and Gilmore, T. D. (2001) *Biochim. Biophys. Acta* **1538,** 260–272
5. Kassel, O., Schneider, S., Heilbock, C., Litfin, M., Göttlicher, M., and Herrlich, P. (2004) *Genes Dev.* **18,** 2518–2528
6. Zhao, M. K., Wang, Y., Murphy, K., Yi, J., Beckerle, M. C., and Gilmore, T. D. (1999) *Gene Expr.* **8,** 207–217
7. Xu, J., Lai, Y. J., Lin, W. C., and Lin, F. T. (2004) *J. Biol. Chem.* **279,** 10459–10468
8. Wada, T., Nakashima, T., Hiroshi, N., and Penninger, J. M. (2006) *Trends Mol. Med.* **12,** 17–25
9. Teitelbaum, S. L. (2000) *Science* **289,** 1504–1508
10. Teti, A., Marchisio, P. C., and Zallone, A. Z. (1991) *Am. J. Physiol.* **261,** C1–C7
11. Jurdic, P., Saltel, F., Chabadel, A., and Destaing, O. (2006) *Eur. J. Cell Biol.* **85,** 195–202
12. Soriano, P., Montgomery, C., Geske, R., and Bradley, A. (1991) *Cell* **64,** 693–702
13. Boyce, B. F., Yoneda, T., Lowe, C., Soriano, P., and Mundy, G. R. (1992) *J. Clin. Invest.* **90,** 1622–1627
14. Lowe, C., Yoneda, T., Boyce, B. F., Chen, H., Mundy, G. R., and Soriano, P. (1993) *Proc. Natl. Acad. Sci. U.S.A.* **90,** 4485–4489
15. Lai, Y. J., Chen, C. S., Lin, W. C., and Lin, F. T. (2005) *Mol. Cell Biol.* **25,** 5859–5868
16. Mills, G. B., and Moolenaar, W. H. (2003) *Nat. Rev. Cancer* **3,** 582–591
17. Choi, J. W., Herr, D. R., Noguchi, K., Yung, Y. C., Lee, C. W., Mutoh, T., Lin, M. E., Teo, S. T., Park, K. E., Mosley, A. N., and Chun, J. (2010) *Annu. Rev. Pharmacol. Toxicol.* **50,** 157–186
18. Karagiosis, S. A., and Karin, N. J. (2007) *Biochem. Biophys. Res. Commun.* **357,** 194–199
19. Masiello, L. M., Fotos, J. S., Galileo, D. S., and Karin, N. J. (2006) *Bone* **39,** 72–82
20. Hurst-Kennedy, J., Boyan, B. D., and Schwartz, Z. (2009) *Biochim. Biophys. Acta* **1793,** 836–846
21. Boucharaba, A., Serre, C. M., Grès, S., Saulnier-Blache, J. S., Bordet, J. C., Guglielmi, J., Clézardin, P., and Peyruchaud, O. (2004) *J. Clin. Invest.* **114,** 1714–1725
22. Boucharaba, A., Serre, C. M., Guglielmi, J., Bordet, J. C., Clézardin, P., and Peyruchaud, O. (2006) *Proc. Natl. Acad. Sci. U.S.A.* **103,** 9643–9648
23. David, M., Wannecq, E., Descotes, F., Jansen, S., Deux, B., Ribeiro, J., Serre, C. M., Grès, S., Bendriss-Vermare, N., Bollen, M., Saez, S., Aoki, J., Saulnier-Blache, J. S., Clézardin, P., and Peyruchaud, O. (2010) *PLoS One* **5,** e9741
24. McMichael, B. K., Kotadiya, P., Singh, T., Holliday, L. S., and Lee, B. S. (2006) *Bone* **39,** 694–705
25. McMichael, B. K., and Lee, B. S. (2008) *Exp. Cell Res.* **314,** 564–573
26. Krits, I., Wysolmerski, R. B., Holliday, L. S., and Lee, B. S. (2002) *Calcif. Tissue Int.* **71,** 530–538
27. Destaing, O., Saltel, F., Géminard, J. C., Jurdic, P., and Bard, F. (2003) *Mol. Biol. Cell* **14,** 407–416
28. McMichael, B. K., Wysolmerski, R. B., and Lee, B. S. (2009) *J. Biol. Chem.* **284,** 12266–12275

29. Lee, B. S., Gluck, S. L., and Holliday, L. S. (1999) *J. Biol. Chem.* **274,** 29164–29171
30. McMichael, B. K., Cheney, R. E., and Lee, B. S. (2010) *J. Biol. Chem.* **285,** 9506–9515
31. Lee, B. S., Holliday, L. S., Krits, I., and Gluck, S. L. (1999) *J. Bone Miner. Res.* **14,** 2127–2136
32. Yi, J., Kloeker, S., Jensen, C. C., Bockholt, S., Honda, H., Hirai, H., and Beckerle, M. C. (2002) *J. Biol. Chem.* **277,** 9580–9589
33. Bai, C. Y., Ohsugi, M., Abe, Y., and Yamamoto, T. (2007) *J. Cell Sci.* **120,** 2828–2837
34. Chastre, E., Abdessamad, M., Kruglov, A., Bruyneel, E., Bracke, M., Di Gioia, Y., Beckerle, M. C., van Roy, F., and Kotelevets, L. (2009) *FASEB J.* **23,** 916–928
35. Chellaiah, M. A. (2006) *Eur. J. Cell Biol.* **85,** 311–317
36. Ory, S., Brazier, H., Pawlak, G., and Blangy, A. (2008) *Eur. J. Cell Biol.* **87,** 469–477
37. Saltel, F., Destaing, O., Bard, F., Eichert, D., and Jurdic, P. (2004) *Mol. Biol. Cell* **15,** 5231–5241
38. E, S., Lai, Y. J., Tsukahara, R., Chen, C. S., Fujiwara, Y., Yue, J., Yu, J. H., Guo, H., Kihara, A., Tigyi, G., and Lin, F. T. (2009) *J. Biol. Chem.* **284,** 14558–14571
39. Prasad, T. S., Kandasamy, K., and Pandey, A. (2009) *Methods Mol. Biol.* **577,** 67–79
40. Nakamura, I., Jimi, E., Duong, L. T., Sasaki, T., Takahashi, N., Rodan, G. A., and Suda, T. (1998) *J. Biol. Chem.* **273,** 11144–11149
41. Honda, H., Oda, H., Nakamoto, T., Honda, Z., Sakai, R., Suzuki, T., Saito, T., Nakamura, K., Nakao, K., Ishikawa, T., Katsuki, M., Yazaki, Y., and Hirai, H. (1998) *Nat. Genet.* **19,** 361–365